

See discussions, stats, and author profiles for this publication at: <https://www.researchgate.net/publication/317557310>

FeNiSiBP glassy alloys with tunable and attractive magnetic performance

Article in *Journal of Non-Crystalline Solids* · June 2017

DOI: 10.1016/j.jnoncrysol.2017.06.008

CITATIONS

0

READS

50

9 authors, including:



Qiu Keqiang

Shenyang University of Technology

146 PUBLICATIONS 727 CITATIONS

[SEE PROFILE](#)



Anding Wang

City University of Hong Kong

38 PUBLICATIONS 230 CITATIONS

[SEE PROFILE](#)



Chuntao Chang

Ningbo Institute of Materials Technology and...

107 PUBLICATIONS 1,573 CITATIONS

[SEE PROFILE](#)

Some of the authors of this publication are also working on these related projects:



Mg alloy [View project](#)



Soft magnetic material [View project](#)

All content following this page was uploaded by [Anding Wang](#) on 15 June 2017.

The user has requested enhancement of the downloaded file.



Contents lists available at ScienceDirect

Journal of Non-Crystalline Solids

journal homepage: www.elsevier.com/locate/jnoncrysol

FeNiSiBP glassy alloys with tunable and attractive magnetic performance

Jing Pang^a, Keqiang Qiu^{a,*}, Fengyu Kong^b, Anding Wang^{c,e,*}, Xiaofeng Liang^a, Chengjuan Wang^a, Chuntao Chang^{c,d}, Xinmin Wang^{c,d}, Chain-Tsuan Liu^e^a School of Materials Science and Engineering, Shenyang University of Technology, Shenyang, Liaoning 110870, China^b School of Materials and Chemical Engineering, Ningbo University of Technology, Ningbo 315016, China^c Key Laboratory of Magnetic Materials and Devices, Ningbo Institute of Materials Technology and Engineering, Chinese Academy of Sciences, Ningbo, Zhejiang 315201, China^d Zhejiang Province Key Laboratory of Magnetic Materials and Application Technology, Ningbo Institute of Materials Technology and Engineering, Chinese Academy of Sciences, Ningbo 315201, China^e Centre for Advanced Structural Materials, Department of Mechanical and Biomedical Engineering, City University of Hong Kong, Tat Chee Avenue, Kowloon Tong, Kowloon, Hong Kong, China

ARTICLE INFO

Keywords:

FeNi-based
Glassy alloy
Glass forming ability
Soft-magnetic property
Anti-corrosion

ABSTRACT

We report a new $(\text{Fe}_{1-x}\text{Ni}_x)_{78}\text{Si}_4\text{B}_{13}\text{P}_5$ ($x = 0-0.8$) alloys with high AFA and stability of super cooled liquid region. By tuning the ratio of Fe and Ni based on the $\text{Fe}_{78}\text{Si}_4\text{B}_{13}\text{P}_5$ alloys, these alloys exhibit tunable and attractive performance is obtained, containing tunable B_s of 0–1.57 T, low H_c of 2.1–0.7 A/m, high μ_e of $9-25 \times 10^3$ and obviously improved anti-corrosion which meets the requirement of most electric devices. These alloys with similar manufacturability are promising candidates for the application as soft-magnetic materials in electric devices and brazing materials.

1. Introduction

Glassy alloys have aroused wide interests from scientific and technological fields [1], because of their unique microstructure and excellent magnetic, mechanic, chemical properties, etc. After half century development [2], a series of alloy systems with large composition range exhibiting unique characteristics were developed [3,4]. Thereinto, the soft-magnetic glassy alloys based on Fe, Co, Ni and their combination are the most widely used in electric and electron devices [5], because of their excellent magnetic performance including high effective permeability (μ_e), high saturation flux density (B_s), low coercivity (H_c) and core loss. However, the widely selective composition and characteristics are always two-edged swords which make us hard to choose and deeply recognize [6]. Take the referenced alloys in this study as an example, the Fe-based alloys [7], FeNi-based [8] and Ni(Fe)-based glassy alloys [9,10], with representative compositions of $\text{Fe}_{78}\text{Si}_9\text{B}_{13}$, $\text{Fe}_{40}\text{Ni}_{38}\text{Mo}_4\text{Si}_6\text{B}_{12}$ and $\text{Ni}_{77}\text{Fe}_3\text{Cr}_{15}\text{Si}_3\text{B}_2$, exhibit outstanding merits and has been widely used in correlated fields shown in Fig. 1. In some electric devices, the merits and demerits of these alloys are equally prominent, which should be balanced and tunable. Tailoring the performance and disclose the compositional effect are extremely desired. In addition, development of a new alloys system with higher glass

forming ability (AFA) and thermal stability than the currently used FeSiB and FeNiMoSiB are also a hotspot [11–15].

Great efforts have been devoted to developing glassy alloys with high AFA and tunable performance [8,11]. It is proved that adjusting the ratios of Fe, Co and Ni is an effective way for magnetic properties tailoring in glassy alloys. However, the attempts in the FeSiB and FeNiMoSiB alloys mentioned above are limited by the low AFA and/or manufacturability. Shen et al. developed (Fe, Co, Ni)BSiNb alloys with high AFA which can be casted into rod samples and investigated the effect of magnetic element ratio detailedly [4,16]. Zhang et al. developed (Fe, Co, Ni)MoPCBSi bulk glassy alloys [17,18]. However, the introduction of metallic element with large atomic size like Nb, Mo, Ta and etc. decreases the B_s [13,19]. In addition, these alloys with low Fe content and refractory elements exhibit quite different production process, compared with the widely produced FeSiB alloys. Therefore, the most feasible and acceptable way to solve this problem is to design new alloy systems based on the industrially mature FeSiB alloys.

In this study, we reported a new alloy system of FeNiSiBP, which exhibits high AFA, B_s , μ_e and low H_c . By tuning the ratio of Fe and Ni based on the $\text{Fe}_{78}\text{Si}_4\text{B}_{13}\text{P}_5$ alloys which can be made into bulk or thick ribbon samples, the tunable and attractive performance was systematically investigated. The compositional effect and property tuning

* Correspondence to: K. Qiu, School of Materials Science and Engineering, Shenyang University of Technology, Shenyang, Liaoning 110870, China.

** Correspondence to: A. Wang, Key Laboratory of Magnetic Materials and Devices, Ningbo Institute of Materials Technology and Engineering, Chinese Academy of Sciences, Ningbo, Zhejiang 315201, China.

E-mail addresses: kqiu@163.com (K. Qiu), anding@nimte.ac.cn (A. Wang).<http://dx.doi.org/10.1016/j.jnoncrysol.2017.06.008>Received 13 February 2017; Received in revised form 31 May 2017; Accepted 5 June 2017
0022-3093/ © 2017 Published by Elsevier B.V.

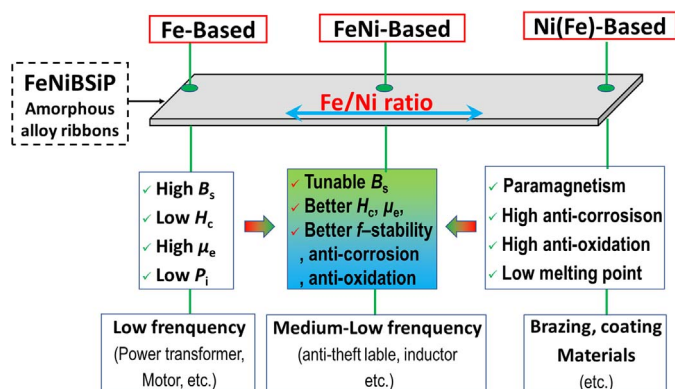


Fig. 1. Illustration of category, tunable property and application of glassy alloy ribbons with different Fe/Ni ratio.

mechanisms discussed in this paper will be good references for the material scientists and engineers. This alloy system is a promising candidate for the application.

2. Experiment procedures

Multi-component alloys with nominal compositions of $(\text{Fe}_{1-x}\text{Ni}_x)_{78}\text{Si}_4\text{B}_{13}\text{P}_5$ ($x = 0, 0.1, 0.2, 0.4, 0.5, 0.6$ and 0.8) were prepared by induction melting with the mixtures of pure Fe (99.99 mass %), Si (99.99 mass%), B (99.5 mass%), Ni (99.9 mass%) and pre-alloyed Fe_3P in an Argon atmosphere. Glassy alloy ribbons with width of about 1 mm and thickness of about $23 \mu\text{m}$ were prepared by single copper roller melt-spinning process. The amorphous structures were clearly identified by X-ray diffraction (XRD) with Cu $K\alpha$ radiation. Crystallization behaviors and thermal physical parameters containing Curie temperature (T_c) and crystallization temperature (T_x) of the glassy alloy were analyzed by differential scanning calorimetry (DSC) at a heating rate of 0.67 K/s . The liquid temperature (T_l) was tested with a DSC at a cooling rate of 0.067 K/s to reduce the influence of undercooling. As the magnetic properties depend on the sample sizes, ribbon samples with similar size mentioned above were used for measurement. The mass of samples was measured by using an electronic balance with high accuracy of $\pm 10^{-5} \text{ g}$ and the density of the master alloys were obtained by Archimedes method. All mass and density values were averaged by multiple tests in order to ensure the accuracy. The intrinsic magnetic properties including B_s and H_c were measured by a vibrating sample magnetometer (VSM) under an applied field of 800 kA/m and a DC $B-H$ loop tracer, respectively. A bending machine was used to test the bending ductility. Ribbon samples were annealed for 10 min by using an isothermal furnace under a low pressure of about $5 \times 10^{-3} \text{ Pa}$ to reduce the influence of inner stress on the above-mentioned properties for the instigation of the relaxation process. Electrochemical measurements were conducted by adopting an electrochemical workstation (AUTOLAB PGSTAT 302) with high sensitivity, in a three-electrode cell using a platinum counter electrode and an Ag/AgCl reference electrode. Potentiodynamic polarization curves were measured at a potential sweep rate of 50 mV/min after open-circuit immersion for about 20 min when the open-circuit potential became almost steady. Prior to electrochemical tests, all samples were polished with metallographic sandpaper of 2000 grain size, washed in ethanol, and dried in air for 24 h. All electrochemical measurements were repeated 3–5 times for reliability and repeatability. All the magnetic and mechanic property measurements were carried out at room temperature.

3. Results and discussion

First, the AFA of the $(\text{Fe}_{1-x}\text{Ni}_x)_{78}\text{Si}_4\text{B}_{13}\text{P}_5$ ($x = 0, 0.2, 0.4, 0.6$ and 0.8) alloys was evaluated. As it has been proved, the alloys closed the eutectic point are more prone to exhibit high AFA [20,21]. We

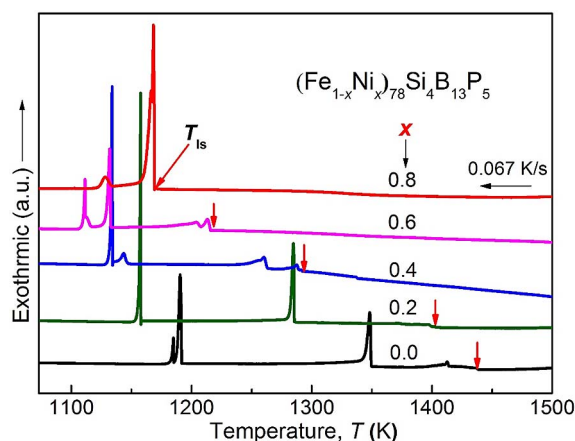


Fig. 2. DSC curves of the $(\text{Fe}_{1-x}\text{Ni}_x)_{78}\text{Si}_4\text{B}_{13}\text{P}_5$ master alloys showing the solidification process.

studied the solidification process of the master alloys by DSC with low cooling rate of 0.067 K/s . As shown in Fig. 2, the onset temperature of the primary exothermic event marked by T_{Is} on DSC solidification curves decreases gradually with the increase of Ni content. The T_{Is} of the alloys with $x = 0.8$ is about 300 K lower than the $\text{Fe}_{78}\text{Si}_4\text{B}_{13}\text{P}_5$ alloy which exhibits high AFA and has been casted into rod samples with maximum diameter of 1.5 mm [11]. In addition, the temperature interval of exothermic peaks decreases markedly from larger than 240 K to about 50 K . It is also seen that the intensity of the first crystallization peak increases and the number of crystallization peaks decrease, indicating a stronger competing effect for the precipitation [22,23]. All these indicate that the alloys toward the eutectic point [24] with the substitution of Fe by Ni. According to the glass forming theory, the alloys closed to the eutectic point and with low T_{Is} favor the formation of amorphous structure, from the thermodynamic and kinetic points [25]. We can hence deduce the alloys with Ni substitution keep high AFA, which is confirmed through preparing fully amorphous ribbons with thickness higher than $60 \mu\text{m}$ by using a low spinning speed of 15 m/s . The high AFA is also proved by the glassy plate samples with thickness larger than 0.5 mm obtained in the gap of the cooling copper mold of the master alloy melting equipment. As the melt spinning and copper mold casting are quite different processes for glassy alloy sample preparation, the AFA is not subjected to evaluate by dimension of the cast samples in this study.

Glassy alloy ribbons were then prepared for the investigation of thermal stability, magnetic properties and anti-corrosion. In order to eliminate the influence of amorphicity, all the $(\text{Fe}_{1-x}\text{Ni}_x)_{78}\text{Si}_4\text{B}_{13}\text{P}_5$ ($x = 0, 0.2, 0.4, 0.6$ and 0.8) glassy alloy ribbons were spun at a wheel velocity of 40 m/s which is much higher than the critical values, exhibiting good surface quality and bending ductility. The amorphous structures were identified by XRD for all ribbon samples. As shown in Fig. 3, the XRD patterns exhibit only diffuse halos without any sharp peak in each pattern.

DSC curves of $(\text{Fe}_{1-x}\text{Ni}_x)_{78}\text{Si}_4\text{B}_{13}\text{P}_5$ ($x = 0-0.8$) glassy alloys were shown in Fig. 4. All samples exhibit glass transition, followed by a supercooled liquid region and then crystallization. With the increase of Ni content, the glassy transition temperature (T_g) decreases gradually from 769 K to 696 K and the onset temperature of crystallization (T_x) decreases from 792 to 735 K . As a result, the temperature interval of the supercooled liquid region (ΔT_x) increases remarkably from 23 to 39 K . It is also clear that the difference of specific heat (ΔC_p) at the glass transition region increase drastically, indicating that the alloys with Ni addition exhibit much higher thermal stability of the supercooled liquid [26]. It is worthy to mention that one exothermic peak changes into two exothermic peaks correlated to two separated crystallization events, for the alloys with Ni content higher than 0.5 . For the alloys with $x = 0-0.5$, only one distinct crystallization exothermic peak indicates

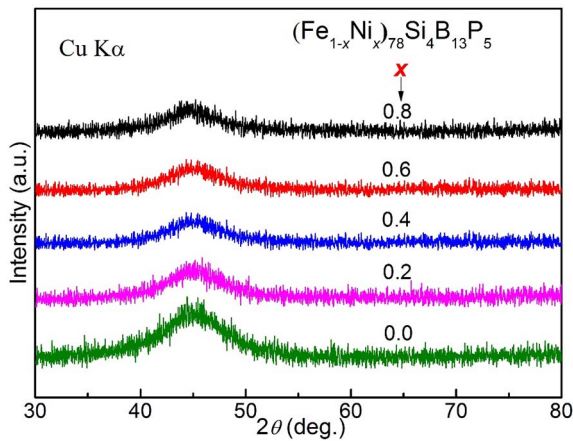


Fig. 3. XRD patterns of the $(\text{Fe}_{1-x}\text{Ni}_x)_{78}\text{Si}_4\text{B}_{13}\text{P}_5$ glassy alloy ribbons melt spun with common process.

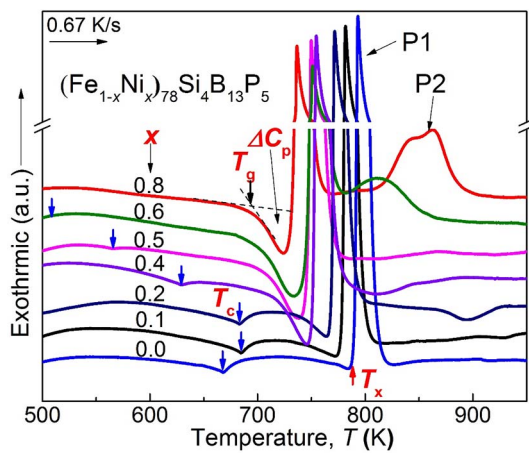


Fig. 4. DSC curves of the $(\text{Fe}_{1-x}\text{Ni}_x)_{78}\text{Si}_4\text{B}_{13}\text{P}_5$ glassy alloy ribbons.

the competing precipitation of crystalline phases [23]. The primary crystallization phase of the high Ni content alloys may be more complicated, consistent with the reports in other alloy systems [27]. Last, we focus on the Curie temperature (T_c), which increases for the alloys with $x = 0.1$ – 0.2 and then drastically decreases with the increase of Ni content. The changes of endothermic valley correlated to the ferromagnetic-paramagnetic transition follow the T_c . All these illustrate that the minor substitution of Ni enhances the magnetic interaction and stability of magnetic properties. No clear T_c can be seen on the DSC curve of the alloy with $x = 0.8$, indicating the paramagnetic nature at room temperature.

All alloy ribbons were then subjected to annealing and the magnetic properties were then investigated systematically. Fig. 5 shows the hysteresis loops measured with VSM for the samples annealed for 10 min at commonly used T_g – 50 K. Except the alloys with $x = 0.8$, all samples exhibit typical hysteresis loops of soft-magnetic materials. The paramagnetic nature at room temperature of the alloy with $x = 0.8$ is verified. The inset shows the Ni content dependence of B_s . The B_s can be tuned from 1.57 T to 0.05 T with Ni content increases from 0 to 0.8 for $(\text{Fe}_{1-x}\text{Ni}_x)_{78}\text{Si}_4\text{B}_{13}\text{P}_5$ alloys. Compared with the referenced $\text{Fe}_{78}\text{Si}_9\text{B}_{13}$ [7] and $\text{Fe}_{40}\text{Ni}_{38}\text{Mo}_4\text{Si}_6\text{B}_{12}$ [14] alloys, the $(\text{Fe}_{1-x}\text{Ni}_x)_{78}\text{Si}_4\text{B}_{13}\text{P}_5$ alloys with the same Ni content for all application fields exhibit higher B_s . It should be noted that the alloys with Ni content higher than 0.8 are good candidate or basic composition for brazing and coating materials, because of the paramagnetic nature, high AFA, low cost and melting point [10].

Because of the paramagnetic nature, the alloy with $x = 0.8$ cannot be used as magnetic materials, which is hence not studied subsequently.

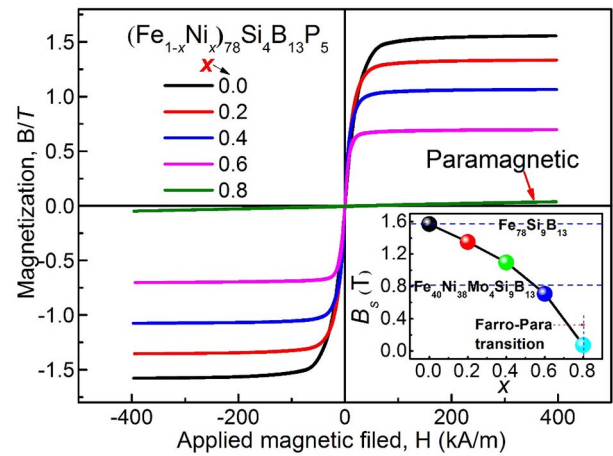


Fig. 5. Hysteresis loops of the glassy alloy ribbons measured with VSM.

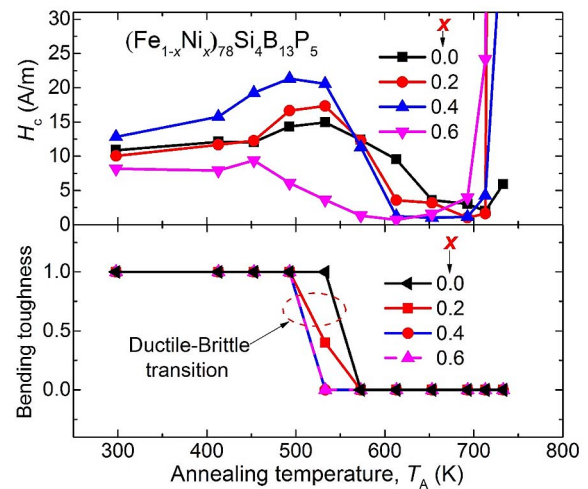


Fig. 6. Annealing temperature (T_A) dependence of H_c and the bending ductility of $(\text{Fe}_{1-x}\text{Ni}_x)_{78}\text{Si}_4\text{B}_{13}\text{P}_5$ glassy alloy ribbons annealed for 10 min.

Fig. 6(a) shows the annealing temperature (T_A) dependence of H_c for $(\text{Fe}_{1-x}\text{Ni}_x)_{78}\text{Si}_4\text{B}_{13}\text{P}_5$ ($x = 0, 0.2, 0.4, 0.6$) glassy alloy ribbons annealed for 10 min. For all the glassy alloys, H_c decreases at the temperature interval of T_c and T_g and reaches the lowest value, which can be attributed to the stress releasing. It should be noted that all glassy alloys exhibit a very low H_c of only 2.1 A/m, 1.1 A/m, 1.0 A/m, 0.7 A/m, respectively, which are also better than the referenced $\text{Fe}_{78}\text{Si}_9\text{B}_{13}$ [6] and $\text{Fe}_{40}\text{Ni}_{38}\text{Mo}_4\text{Si}_6\text{B}_{12}$ alloys [14]. The good softness is considered to originate from the high degree of amorphicity due to high AFA and the thorough relaxation of stress [28].

After magnetic property tests, all samples were then subjected to bending ductility test which was detailedly investigated in the former works [29]. To ensure the repeatability and accuracy, five ribbons with the same annealing state were tested and an average value was used. As shown in Fig. 6(b), the substitution of Ni decreases the ductile-brittle transition temperature (T_{DB}) slightly. The basic $\text{Fe}_{78}\text{Si}_4\text{B}_{13}\text{P}_5$ glassy alloy exhibits similar T_{DB} with the commonly used $\text{Fe}_{78}\text{Si}_9\text{B}_{13}$ alloy which has been widely studied and acceptable for applications [30]. For the major Ni addition, we can also improve the ductility by annealing at low temperature for long time, because of the low T_c .

Fig. 7 shows the frequency dependence of μ_e under a field of 1 A/m for the $(\text{Fe}_{1-x}\text{Ni}_x)_{78}\text{Si}_4\text{B}_{13}\text{P}_5$ ($x = 0, 0.2, 0.4, 0.6$) glassy alloy ribbons annealed at the optimum conditions. It is clear that the introduction of Ni increase the μ_e at 400 Hz drastically from 9×10^3 to 25×10^3 . The high Ni content alloys also exhibit excellent μ_e frequency-stability, which keeps high value 10×10^3 in large frequency

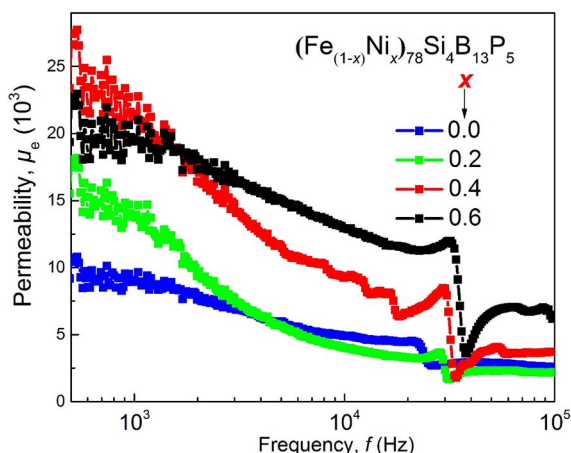


Fig. 7. Effective permeability (μ_e) as a function of frequency for the glassy alloy ribbons annealed for 10 min at optimal temperature.

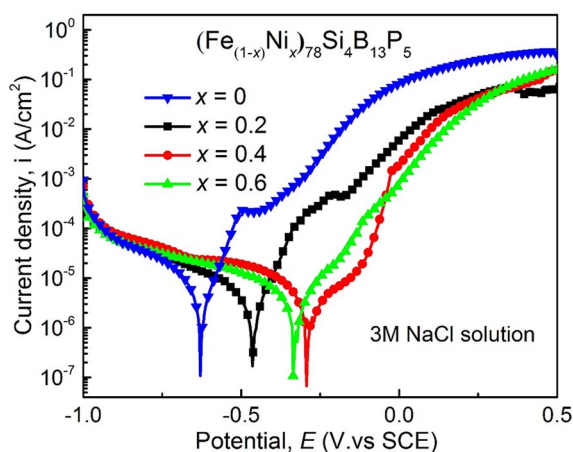


Fig. 8. Potentiodynamic polarization curves of the $(\text{Fe}_{1-x}\text{Ni}_x)_{78}\text{Si}_4\text{B}_{13}\text{P}_5$ glassy alloy ribbons in 3 M NaCl solution open to air at 298 K.

range until the cut-up frequency. The $\text{Fe}_{78}\text{Si}_4\text{B}_{13}\text{P}_5$ glassy alloy exhibits similar μ_e with the $\text{Fe}_{78}\text{Si}_9\text{B}_{13}$ alloy at low frequency range. The high Ni content alloys exhibit higher μ_e than the referenced $\text{Fe}_{40}\text{Ni}_{38}\text{Mo}_4\text{Si}_6\text{B}_{12}$ alloy [14].

As the soft-magnetic materials often used in different environment, corrosion resistance is considered as an indication of the durability of the soft-magnetic material. Fig. 8 shows potentiodynamic polarization curves of the $(\text{Fe}_{1-x}\text{Ni}_x)_{78}\text{Si}_4\text{B}_{13}\text{P}_5$ ($x = 0, 0.2, 0.4, 0.6$) glassy alloy ribbons in 3 M NaCl solution open to air at 298 K. These alloys without metallic element addition do not exhibit an obvious active-passive transition in 3 M NaCl solution, consistent with former reports of FeSiB and FeSiBP alloys [31]. However, the corrosion potential greatly increases from -0.62 to -0.29 V vs. SCE, with the Ni content increase from 0 to 0.4. In this work, the further increase of Ni content does not further increase the corrosion potential. This shows that the anti-corrosion is obviously improved. According to the results of simple water immersion test, a lot of rust dots is found on the surface of the $\text{Fe}_{78}\text{Si}_4\text{B}_{13}\text{P}_5$ alloy ribbons after 1 day, but no rust dots can be seen on $(\text{Fe}_{1-x}\text{Ni}_x)_{78}\text{Si}_4\text{B}_{13}\text{P}_5$ alloy ribbons with $x = 0.4-0.6$ even after 1 week. Therefore, we can declare that the improvement of anti-corrosion of P added Fe-based alloys is necessary and the anti-corrosion of the Ni added alloys in this work in quite good for the application in electric devices.

To sum up, the gradually improved μ_e and f -stability, decreased H_c and B_s , enhanced anti-corrosion, together with the high manufacturability owing to the high AFA and low cost, make $(\text{Fe}_{1-x}\text{Ni}_x)_{78}\text{Si}_4\text{B}_{13}\text{P}_5$ ($x = 0, 0.2, 0.4, 0.6$) glassy alloys an attractive

candidate for applications in a variety of electric devices. The gradual change of the magnetic properties and the anti-corrosion explored detailedly in this work will give a useful guide for the future choice. Here, we should also mention that the Ni and Fe are metallurgically similar elements. The substitution will not change the ribbon production process substantially, which is quite important for the industrial production and will make the performance tailing more meaningful.

Finally, we discuss the origin of the attractive and tunable properties of the $(\text{Fe}_{1-x}\text{Ni}_x)_{78}\text{Si}_4\text{B}_{13}\text{P}_5$ ($x = 0, 0.2, 0.4, 0.6$ and 0.8) glassy alloys. The pronounced improvement of AFA for $\text{Fe}_{78}\text{Si}_4\text{B}_{13}\text{P}_5$ alloy, compared with $\text{Fe}_{78}\text{Si}_9\text{B}_{13}$ alloy [11,13], has been explained from the aspects of bonding nature and entropy. Because P contains more s electrons and larger negative value of mixing enthalpies [32] with Fe, the substitution of Si by P leads to the enhancement of s-d hybrid bonding [33] and stronger atomic interaction, which can enhance the viscosity of supercooled liquid alloys and is helpful to the improvement of GFA. Here, we focus on the Ni substitution effect. As similar elements, the substitution of Fe by Ni makes the alloys more closed to the eutectic point, as shown in Fig. 2. The stability of the supercooled liquid alloys is obviously enhanced and the crystallization phase becomes more complicated, as shown in Fig. 4. Together with the increased entropy by new element introduction, the alloys thermodynamically and kinetically favor the formation of glassy phase [24,25]. The tuning of magnetic properties can be explained by the less 3d electrons which lead to lower Bohr magneton number and B_s , as well as lower magnetostriction and magnetic anisotropy of the FeNi-based glassy alloys which lead to easier magnetization process and better soft-magnetic properties [34]. The improvement of the anti-corrosion can be attributed to the much higher chemical stability of the Ni than Fe.

4. Conclusion

FeNiSiBP glassy alloys with tunable and attractive performance were developed. The effects of Ni substitution of Fe on AFA, magnetic properties, bending ductility and anti-corrosion of FeSiBP glassy alloy ribbons were investigated. The main results are summarized as follows:

1. The $(\text{Fe}_{1-x}\text{Ni}_x)_{78}\text{Si}_4\text{B}_{13}\text{P}_5$ ($x = 0, 0.2, 0.4, 0.6$ and 0.8) alloys have high AFA and stability of supercooled liquid region.
2. The $(\text{Fe}_{1-x}\text{Ni}_x)_{78}\text{Si}_4\text{B}_{13}\text{P}_5$ ($x = 0, 0.2, 0.4, 0.6$ and 0.8) alloys exhibit excellent soft-magnetic properties, containing tunable B_s of 0–1.57 T, low H_c of 2.1–0.7 A/m, high μ_e of $9-25 \times 10^3$. The Ni added alloys also exhibit better frequency-magnetic properties stability.
3. With the introduction of Ni, the corrosion potential increases greatly from -0.62 to -0.29 V vs. SCE. The anti-corrosion is obviously improved and meet the requirement of most electric devices.

Acknowledgements

This work was mainly supported by the National Natural Science Foundation of China (Grant No. 51601206, 51601101), Ningbo International Cooperation Projects (Grant No. 2015D10022) and Ningbo Major Project for Science and Technology (Grant No. 2014 01B1003003).

References

- [1] A. Inoue, A. Takeuchi, Recent development and application products of bulk glassy alloys, *Acta Mater.* 59 (2011) 2243–2267.
- [2] P. Duwez, S.C.H. Lin, Amorphous ferromagnetic phase in iron-carbon-phosphorus alloys, *J. Appl. Phys.* 38 (1967) 4096–4097.
- [3] A. Inoue, X.M. Wang, W. Zhang, Developments and applications of bulk metallic glasses, *Rev. Adv. Mater. Sci.* 18 (2008) 1–9.
- [4] H. Gao, R. Xiang, S.X. Zhou, B.S. Dong, Y.G. Wang, The influence of P on glass forming ability and clusters in melt of FeSiBP amorphous soft-magnetic alloy, *J. Mater. Sci. Mater. Electron.* 26 (2015) 7804–7810.
- [5] G. Herzer, Modern soft magnets: amorphous and nanocrystalline materials, *Acta*

- Mater. 61 (2013) 718–734.
- [6] A.D. Wang, C.L. Zhao, A.N. He, H. Men, C.T. Chang, X.M. Wang, Composition design of high Bs Fe-based amorphous alloys with good amorphous-forming ability, *J. Alloys Compd.* 656 (2016) 729–734.
- [7] M. Mouhamad, C. Elleau, F. Mazaleyrat, C. Guillaume, B. Jarry, Physicochemical and accelerated aging tests of Metglas 2605SA1 and Metglas 2605HB1 amorphous ribbons for power applications, *IEEE Trans. Magn.* 47 (2011) 3192–3195.
- [8] T.D. Shen, R.B. Schwarz, Bulk ferromagnetic glasses in the Fe-Ni-P-B system, *Acta Mater.* 49 (2001) 837–847.
- [9] T.A. Zimogliadova, E.A. Drobyaz, M.G. Golkovskii, V.A. Bataev, V.G. Durakov, N.Y. Cherkasova, Investigation of Ni-Cr-Si-Fe-B coatings produced by the electron beam cladding technique, *IOP Conference Series: Materials Science and Engineering* 156 (2016) 012017.
- [10] J. Skamat, O. Cernasejus, A.V. Valiulis, R. Lukauskaite, N. Visniakov, Improving hardness of Ni-Cr-Si-B-Fe-C thermal sprayed coatings through grain refinement by vibratory treatment during refusion, *Mater. Sci.-Medziagotyra* 21 (2015) 207–214.
- [11] J.H. Zhang, C.T. Chang, A.D. Wang, B.L. Shen, Development of quaternary Fe-based bulk metallic glasses with high saturation magnetization above 1.6 T, *J. Non-Cryst. Solids* 358 (2012) 1443–1446.
- [12] A. Makino, C.T. Chang, T. Kubota, A. Inoue, Soft magnetic Fe-Si-B-P-C bulk metallic glasses without any glass-forming metal elements, *J. Alloys Compd.* 483 (2009) 616–619.
- [13] A. Makino, T. Kubota, C. Chang, M. Makabe, A. Inoue, FeSiBP bulk metallic glasses with high magnetization and excellent magnetic softness, *J. Magn. Magn. Mater.* 320 (2008) 2499–2503.
- [14] A.D. Wang, M.X. Zhang, J.H. Zhang, H. Men, B.L. Shen, S.J. Pang, T. Zhang, FeNiPBNb bulk glassy alloys with good soft-magnetic properties, *J. Alloys Compd.* 536 (2012) S354–S358.
- [15] A. Wang, C. Zhao, A. He, S. Yue, C. Chang, B. Shen, X. Wang, R.-W. Li, Development of FeNiNbSiBP bulk metallic glassy alloys with excellent magnetic properties and high glass forming ability evaluated by different criteria, *Intermetallics* 71 (2016) 1–6.
- [16] C. Chang, B. Shen, A. Inoue, Synthesis of bulk glassy alloys in the (Fe,Co,Ni)-B-Si-Nb system, *Mater. Sci. Eng. A* 449 (2007) 239–242.
- [17] M.X. Zhang, A.D. Wang, B.L. Shen, Enhancement of glass-forming ability of Fe-based bulk metallic glasses with high saturation magnetic flux density, *AIP Adv.* 2 (2012) 7.
- [18] M. Zhang, F. Kong, A. Wang, C. Chang, B. Shen, Soft magnetic properties of bulk FeCoMoPCBSi glassy core prepared by copper mold casting, *J. Appl. Phys.* 111 (2012) 07A312-313.
- [19] C.T. Chang, B.L. Shen, A. Inoue, FeNi-based bulk glassy alloys with superhigh mechanical strength and excellent soft-magnetic properties, *Appl. Phys. Lett.* 89 (2006) 051912.
- [20] A.R. Yavari, Solving the puzzle of eutectic compositions with ‘miracle glasses’, *Nat. Mater.* 4 (2005) 2–3.
- [21] Z.P. Lu, C.T. Liu, A new glass-forming ability criterion for bulk metallic glasses, *Acta Mater.* 50 (2002) 3501–3512.
- [22] M.X. Xia, S.G. Zhang, C.L. Ma, J.G. Li, Evaluation of glass-forming ability for metallic glasses based on order-disorder competition, *Appl. Phys. Lett.* 89 (2006) 091917.
- [23] Z.P. Lu, D. Ma, C.T. Liu, Y.A. Chang, Competitive formation of glasses and glass-matrix composites, *Intermetallics* 15 (2007) 253–259.
- [24] Z.P. Lu, C.T. Liu, Glass formation criterion for various glass-forming systems, *Phys. Rev. Lett.* 91 (2003) 115505-115501.
- [25] W.L. Johnson, Thermodynamic and kinetic aspects of the crystal to glass transformation in metallic materials, *Prog. Mater. Sci.* 30 (1986) 81–134.
- [26] A. Inoue, Stabilization of metallic supercooled liquid and bulk amorphous alloys, *Acta Mater.* 48 (2000) 279–306.
- [27] A.D. Wang, Q.K. Man, M.X. Zhang, H. Men, B.L. Shen, S.J. Pang, T. Zhang, Effect of B to P concentration ratio on glass-forming ability and soft-magnetic properties in $(\text{Fe}_{0.5}\text{Ni}_{0.5})_{0.78}\text{B}_{0.22} - \text{P}_x\text{Nb}_3$ glassy alloys, *Intermetallics* 20 (2012) 93–97.
- [28] T. Bitoh, A. Makino, A. Inoue, Origin of low coercivity of $(\text{Fe}_{0.75}\text{B}_{0.15}\text{Si}_{0.10})_{100-x}\text{Nb}_x$ ($x = 1-4$) glassy alloys, *J. Appl. Phys.* 99 (2006) 08F102.
- [29] X. Liang, A. He, A. Wang, J. Pang, C. Wang, C. Chang, K. Qiu, X. Wang, C.-T. Liu, Fe content dependence of magnetic properties and bending ductility of FeSiBPC amorphous alloy ribbons, *J. Alloys Compd.* 694 (2017) 1260–1264.
- [30] Y.C. Niu, X.F. Bian, W.M. Wang, Origin of ductile–brittle transition of amorphous $\text{Fe}_{78}\text{Si}_9\text{B}_{13}$ ribbon during low temperature annealing, *J. Non-Cryst. Solids* 341 (2004) 40–45.
- [31] C.T. Chang, C.L. Qin, A. Makino, A. Inoue, Enhancement of glass-forming ability of FeSiBP bulk glassy alloys with good soft-magnetic properties and high corrosion resistance, *J. Alloys Compd.* 533 (2012) 67–70.
- [32] A. Takeuchi, A. Inoue, Classification of bulk metallic glasses by atomic size difference, heat of mixing and period of constituent elements and its application to characterization of the main alloying element, *Mater. Trans.* 46 (2005) 2817–2829.
- [33] H.S. Chen, J.T. Krause, E. Coleman, Elastic-constants, hardness and their implications to flow properties of metallic glasses, *J. Non-Cryst. Solids* 18 (1975) 157–171.
- [34] T. Bitoh, A. Makino, A. Inoue, Origin of low coercivity of Fe-(Al, Ga)-(P, C, B, Si, Ge) bulk glassy alloys, *Mater. Trans.* 44 (2003) 2020–2024.